

# Theoretical investigation on the H sublattice in $\text{CaH}_6$ and energetic performance

Zhihong Huang(黄植泓)<sup>1</sup>, Nan Li(李楠)<sup>1,†</sup>, Jun Zhang(张俊)<sup>2,‡</sup>, Xiuyuan Li(李修远)<sup>1</sup>, Zihuan Peng(彭梓桓)<sup>1</sup>, Chongwen Jiang(江崇文)<sup>1</sup>, and Changqing Jin(靳常青)<sup>2</sup>

<sup>1</sup>State Key Laboratory of Explosion Science and Technology, School of Mechatronic Engineering, Beijing Institute of Technology, Beijing 100081, China

<sup>2</sup>Beijing National Laboratory for Condensed Matter Physics, Institute of Physics, Chinese Academy of Sciences, Beijing 100190, China

(Received 16 April 2025; revised manuscript received 3 June 2025; accepted manuscript online 6 June 2025)

Metal superhydride compounds (MSHCs) have attracted much attention in the fields of high-pressure physics due to the superconductivity properties deriving from the metallic-hydrogen-like characteristics and relatively mild synthesis conditions. However, their energetic performance and related potential applications are still open issues till now. In this study,  $\text{CaH}_6$  and  $\text{NbH}_3$ , which exhibit evidently differences in their geometric and electronic structures, were chosen as examples of MSHCs to investigate their energetic performance. The structure, bonding features and energetic performance of  $\text{CaH}_6$  and  $\text{NbH}_3$  were predicted based on first-principles calculations. Our results reveal that high-pressure MSHCs always exhibit high energy densities. The range of theoretical energy density of  $\text{CaH}_6$  was predicted as 2.3–5.3 times of TNT, while the value for  $\text{NbH}_3$  was predicted as 1.2 times of TNT. Our study further uncover that  $\text{CaH}_6$  has outstanding energetic properties, which are ascribed to the three-dimensional (3D) aromatic H sublattice and the strong covalent bonding between the H atoms. Moreover, the detonation process and products of rapid energy-release stage of  $\text{CaH}_6$  were simulated via AIMD method, based on which its superior combustion performance was predicted and its specific impulse was calculated as 490.66 s. This study not only enhances the chemical understanding of MSHCs, but also extends the paradigm of traditional energetic materials and provides a new route to design novel high energy density materials.

**Keywords:** metal superhydride compounds, energetic performance, first-principles simulation, high pressure

**PACS:** 62.50.–p, 63.90.+t, 65.40.–b, 71.15.Pd

**DOI:** 10.1088/1674-1056/ade1c3

**CSTR:** 32038.14.CPB.ade1c3

## 1. Introduction

Metallic hydrogen has long been sought in the field of high-pressure physics since its first proposal in 1935 by physicists Eugene Wigner and Hillard Huntington,<sup>[1]</sup> with numerous theoretical studies revealing its outstanding properties continuously. In 1968, Ashcroft<sup>[2]</sup> predicted that metallic hydrogen could exhibit superconductivity at room temperature. In 1999, Nellis<sup>[3]</sup> predicted its extremely high energy density, making it a potential candidate for fuel, propellant, or explosive. In 2010, its energy density was predicted as 216 MJ/kg by Silvera *et al.*,<sup>[4]</sup> which is 46.85 times that of trinitrotoluene (TNT) and far exceeds those of widely studied energetic materials such as the most powerful energetic materials hexanitrohexaazaisowurtzitane (CL-20) and 1,3,5,7-tetranitro-1,3,5,7-tetrazocane (HMX). These remarkable predicted properties have propelled the studies of metallic hydrogen to the cutting edge of materials science and high-pressure physics. However, due to the extremely high pressures required, the synthesis and stabilization of metallic hydrogen remain persistent challenges. In 2012, McMahon *et al.*<sup>[5]</sup> theoretically predicted that the synthesis pressure of metallic hydrogen reaches

~ 500 GPa. In 2017, Isaac Silvera *et al.*<sup>[6]</sup> reported the observation of metallic hydrogen under approximately 495 GPa, though great controversies remain.

In 2004, Neils<sup>[7]</sup> proposed the concept of chemical pre-compression, which could lower the formation pressures of metallic hydrogen by introducing other elements, particularly metals. Following this idea, in 2014, Duan *et al.*<sup>[8]</sup> predicted that  $\text{H}_3\text{S}$  could be synthesized under 111 GPa, which was regarded as a milestone of superhydrides and proved by experimental success that  $\text{H}_3\text{S}$  was successfully synthesized under 90 GPa in 2015 by MI Erements.<sup>[9]</sup> Then, scientists have devoted their research to superhydrides, especially metal superhydride compounds (MSHCs), and more and more novel MSHCs have been achieved.<sup>[10–13]</sup> Typically,  $\text{LaH}_{10}$  and  $\text{CaH}_6$  exhibit superconductivity with high- $T_c$  higher than 200 K, similar to that predicted for pure solid-state metallic hydrogen.<sup>[11,12]</sup> Also, the lattices of superhydrides composed of metals near the s–d border and H atoms possess strong covalent H–H networks,<sup>[14,15]</sup> which inspire us to hypothesize their high energy density. On the other hand, the ambient-pressure metal hydrides such as  $\text{AlH}_3$  and  $\text{MgH}_2$  have been widely in-

<sup>†</sup>Corresponding author. E-mail: leen04@bit.edu.cn

<sup>‡</sup>Corresponding author. E-mail: zhang@iphy.ac.cn

© 2025 Chinese Physical Society and IOP Publishing Ltd. All rights, including for text and data mining, AI training, and similar technologies, are reserved.

<http://iopscience.iop.org/cpb> <http://cpb.iphy.ac.cn>

vestigated as energetic materials.<sup>[16–19]</sup> In 2021, Wu *et al.*<sup>[17]</sup> measured the combustion heat of  $\text{MgH}_2$ ,  $\text{TiH}_2$ , and  $\text{ZrH}_2$  with values of 29.96 MJ/kg, 20.94 MJ/kg, and 12.22 MJ/kg, respectively. In 2024, Makhov *et al.*<sup>[19]</sup> reported the addition of Al and  $\text{AlH}_3$  to an explosive could greatly improve its heat and the TNT equivalent of an underwater explosion. Considering these two aspects, MSHCs should be promising candidates for energetic materials.

In recent years, our research team has synthesized a series of hydrogen-rich MSHCs,<sup>[20–22]</sup> such as  $\text{CaH}_6$  and  $\text{Lu}_4\text{H}_{23}$ , using the diamond anvil cell combined with an *in-situ* laser heating technique. Nevertheless, existing studies<sup>[23–26]</sup> on high-pressure MSHCs have predominantly focused on their superconductivity and electron–phonon coupling interactions. To date, their energetic performance has barely been studied, while its comprehension is essential for developing novel energetic materials.

In this work, the detailed energetic performance of  $\text{CaH}_6$  and  $\text{NbH}_3$  was investigated based on the density functional theory (DFT), which were chosen as the typical representative MSHCs due to their differences in structure and chemical bonding. The critical influences on energetic performance imposed by the structures of MSHCs were uncovered. Further investigations reveal that  $\text{CaH}_6$  also possesses high energy density and high specific impulse, highlighting its potential applications as high explosives and propellant components.

## 2. Methods

The original structures of  $\text{CaH}_6$  and  $\text{NbH}_3$  under high pressure are obtained from experimental data,<sup>[20,22]</sup> and are investigated using the Vienna *Ab Initio* Simulation Package (VASP)<sup>[27,28]</sup> afterwards. The projector augmented wave (PAW) method<sup>[29]</sup> with a plane-wave cutoff energy of 400 eV is employed, and the Perdew–Burke–Ernzerhof (PBE) functional within the generalized gradient approximation (GGA)<sup>[30]</sup> is used to describe the exchange–correlation interactions. Considering the strong electron correlation effects in  $\text{NbH}_3$ , the Hubbard parameter  $U$ <sup>[31]</sup> is applied to the effective potential. The effective  $U$  value is set to 2.0 eV for d-orbitals of Nb atoms, as used in the previous literature.<sup>[32]</sup> To account for van der Waals interactions, the DFT-D3 method<sup>[33]</sup> is applied for corrections. The convergence criteria for the Hellmann–Feynman force and energy are set to 0.01 eV/Å and  $1 \times 10^{-5}$  eV, respectively. The  $K$ -point mesh is sampled within  $2\pi \times 0.02 \text{ Å}^{-1}$  using the Gamma scheme in the Brillouin zone. The structures and electron localization function (ELF) of the two MSHCs are visualized using the VESTA ver. 3.90.0a program.<sup>[34]</sup> The integrated crystalline orbital Hamiltonian population (ICOHP) calculations are carried out by employing the LOBSTER ver.5.1.1 program.<sup>[35]</sup>

The calculations of the theoretical detonation parameters of the two high-pressure MSHCs, including heat of detonation ( $Q$ ), detonation velocity ( $D$ ), and detonation pressure ( $P$ ), were conducted following the Hess’s law and Kamlet–Jacobs equations<sup>[36]</sup> as shown below:

$$Q = E(M) + \frac{x}{2}E(\text{H}_2) - E(\text{MH}_x), \quad (1)$$

$$\phi = 0.4885Nm^{\frac{1}{2}}Q^{\frac{1}{2}}, \quad (2)$$

$$D = 1.01\phi^{\frac{1}{2}}(1 + 1.30\rho), \quad (3)$$

$$P = 1.558\phi\rho^2, \quad (4)$$

where  $M = \text{Ca}$  and  $\text{Nb}$ , and  $x = 6$  and  $3$ , respectively;  $\phi$  represents a parameter for energy under detonation conditions,  $N$  (in mol/g) represents the amount of moles of gas products formed per gram of MSHCs during detonation under high pressure,  $m$  is the average molar mass of these gases, which is 2.016 g/mol, and  $\rho$  (in g/cm<sup>3</sup>) denotes the density of the two MSHCs under high pressure. Moreover, the energy densities of the two MSHCs are numerically equal to their  $Q$ , according to the common definition for traditional energetic materials.

The thermal decomposition behavior of  $\text{CaH}_6$  was simulated by AIMD within the CP2K program,<sup>[37]</sup> with the orbital transformation technology<sup>[38]</sup> used to accelerate computing. A  $2 \times 2 \times 2$  supercell of  $\text{CaH}_6$  containing 112 atoms was conducted and optimized under 200 GPa. After optimization, the system was run for 10 ps at 3000 K, and subsequently for 3 ps with cooling to 298.15 K in the constant NPT ensemble at 1 atm under the PBE-D3<sup>[39]</sup> level of theory with the DZVP-MOLOPT-SR-GTH<sup>[40]</sup> basis set. The convergence criteria for forces and energy were set to 0.01 eV/Å and  $1 \times 10^{-5}$  eV, respectively. All simulations were performed under periodic boundary conditions (PBC), and the thermostat was set as CSVR for efficient and accurate temperature control. The time step was 0.5 fs, and the time constant was 200 fs. The DIIS minimizer was employed for all integration calculations in the simulations.

The calculations of combustion performance were carried out by employing the Explo5 ver.6.04 program under isobaric combustion conditions at a chamber pressure of 7 MPa, with equilibrium expansion conditions at the nozzle throat.

## 3. Results and discussion

### 3.1. Structures and bonding features

In this study,  $\text{CaH}_6$  and  $\text{NbH}_3$  were chosen and investigated as examples of MSHCs by employing the first-principle GGA-PBE method. Firstly,  $\text{CaH}_6$  and  $\text{NbH}_3$  were optimized respectively under 150 GPa and 300 GPa. The calculated structures are similar to the experimental structures,<sup>[20,22]</sup> and all the relative errors in lattice parameters are within 5% (as listed in Table S1), indicating the reliability of our computational scheme. High formation pressure always causes the

energy input to systems, and the energy properties of  $\text{CaH}_6$  and  $\text{NbH}_3$  are closely related to the programmed pressure. To eliminate the impact of different programmed pressures, we optimized both structures again at 200 GPa. The structures of  $\text{CaH}_6$  and  $\text{NbH}_3$  under 200 GPa almost remain unchanged, and the detailed structure parameters are listed in Table S2. All following discussions of the structures, energies and properties of  $\text{CaH}_6$  and  $\text{NbH}_3$  are based on the structures at 200 GPa.

As shown in Figs. 1(a) and 1(b), compared to ambient-pressure metal hydrides, MSHCs always have higher H coordination, more complex geometric structures and novel electronic configurations. Besides the interactions between metal and H atoms, the high pressure facilitates to drive the transformation of hydrogen to atomic phases. The H sublattices in MSHCs always feature a strong covalent H–H network and high electron density. We first discuss the geometric structures of  $\text{CaH}_6$  and  $\text{NbH}_3$ .

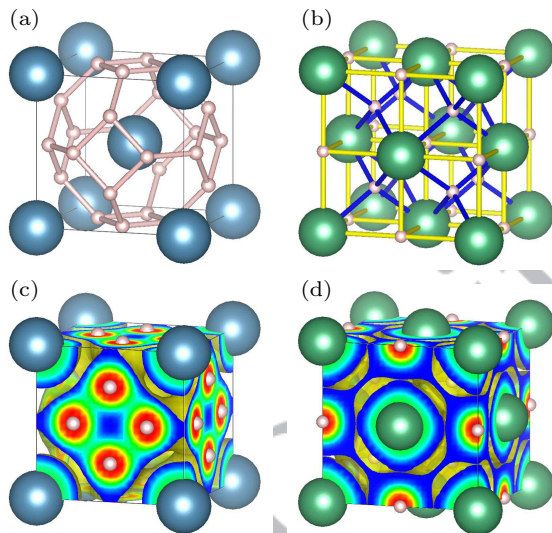


**Fig. 1.** Structures and ELF of high-pressure MSHCs. (a) The structure of  $\text{CaH}_6$  under 200 GPa. (b) The structure of  $\text{NbH}_3$  under 200 GPa. (c) The ELF (isosurface = 0.1) of  $\text{CaH}_6$  under 200 GPa. (d) The ELF (isosurface = 0.1) of  $\text{NbH}_3$  under 200 GPa. The white, blue, and green balls represent the H, Ca, and Nb atoms, respectively. The pink, blue and yellow bonds represent the H–H covalent bonds in  $\text{CaH}_6$ , the Nb–H<sub>Y</sub>-type and Nb–H<sub>Z</sub>-type bonds in  $\text{NbH}_3$ , respectively. The Ca–H bonds are not presented.

Under 200 GPa, the structure of  $\text{CaH}_6$  (shown in Fig. 1(a)) exhibits high symmetry and high hydrogen content. The Ca atoms in  $\text{CaH}_6$  form body-centered cubic (BCC) sublattices, and the uniformly distributed H atoms form a highly symmetric covalent H network. Specifically, each H atom bonds with four adjacent H atoms via equivalent H–H covalent bonds with a bond length of 1.191 Å. Every 24 H atoms constitute a  $\text{H}_{24}$  cage, in which eight  $\text{H}_6$  hexagonal units are located in the tetrahedral interstitial sites and six  $\text{H}_4$  square units are located in the octahedral interstitial sites of the Ca sublattice. In addition, all the distances from the H atoms to the cage-centered Ca atoms in  $\text{CaH}_6$  are 1.883 Å.

$\text{NbH}_3$  (shown in Fig. 1(b)) has an  $\text{XY}_2\text{Z}$ -type Heusler structure, where the Nb atoms occupy the X sites in a face-centered cubic (FCC) arrangement and the H atoms occupy the Y and Z sites. The Y-type and Z-type H atoms in  $\text{NbH}_3$  are individually distributed in the tetrahedral and octahedral interstitial sites of the Nb sublattice, respectively. The bond lengths of Nb–H<sub>Y</sub>-type bond and Nb–H<sub>Z</sub>-type bond are respectively 1.719 Å and 1.985 Å, and the shortest distance between the adjacent H atoms is 1.719 Å.

Further, the electronic structure and bonding features of  $\text{CaH}_6$  and  $\text{NbH}_3$  were investigated via ELF and ICOHP. The ELF, derived from the topological analysis of electron pair probability based on the Pauli exclusion principle, can intuitively display the electron occupation in the MSHCs system.<sup>[41]</sup> And the ICOHP values (commonly negative) can be used to evaluate the interaction strengths between two atoms by integrating the partition of band-structure energy calculated via the Hamiltonian matrix elements weighted densities of states. Specifically, the lower ICOHP value indicates the stronger interaction, while the value close to zero implies no chemical bonding.<sup>[42,43]</sup>

The ELF of  $\text{CaH}_6$  (shown in Fig. 1(c)) shows that there is low electron occupation around Ca atoms and higher electron occupation around H atoms, which implies the electron delocalization and metallization of  $\text{CaH}_6$ . Notably, relatively high electron occupation exists between the adjacent H atoms and expands in the H sublattice of  $\text{CaH}_6$ , which implies an extended H network with covalent H–H bonds. The ICOHP value for H–H bonds (−0.559 eV) is lower than those for Ca–H (−0.126 eV) and Ca–Ca (−0.036 eV) interactions. Both ELF and ICOHP of  $\text{CaH}_6$  reveal the strong H–H covalent bonding, weak interaction between Ca and H atoms and no interaction between Ca atoms.

For  $\text{NbH}_3$  (shown in Fig. 1(d)), the ICOHP values of Nb–H<sub>Y</sub>, Nb–H<sub>Z</sub> and Nb–Nb are respectively −1.201 eV, −0.585 eV and −0.534 eV, which imply the strong bonding interactions of Nb–H and Nb–Nb. The high electron occupation between the Nb and H atoms indicates that Nb–H bonds exhibit a certain degree of covalent character, and both the low electron occupation and the near-zero ICOHP value of −0.040 eV between the adjacent H atoms indicate the weak interactions between them.

Here, we further discuss the performance of H atoms under different pressures. Under ambient pressure, H atoms typically form  $\text{H}_2$  molecules, where the H–H bond is a  $\sigma$ -bond formed by the overlap of the two 1s orbitals of H atoms, with a bond length of 0.74 Å and an ICOHP value of −2.555 eV. The intermolecular distances between  $\text{H}_2$  molecules exceed 3 Å, and their interactions are dominated by dispersion forces. For the traditional metal hydrides at ambient-pressure conditions, such as  $\text{AlH}_3$ , H atoms interact with metal atoms through ionic



bonds, while there is almost no interaction between H atoms. The ELF (Fig. S1) and ICOHP of  $\text{AlH}_3$  indicate that electron occupation mainly locates around H atoms. The ICOHP values for Al–H and H–H are respectively  $-1.309$  eV and  $-0.003$  eV, which means the strong ionic interactions between Al and H atoms but almost no interactions between H atoms.

However, the H atoms behave differently in high-pressure MSHCs. The high pressure increases both the potential energy and kinetic energy of  $\text{CaH}_6$  and  $\text{NbH}_3$  systems, and the kinetic energy increases more quickly than the Coulomb energy with the increase of pressure.<sup>[44]</sup> The increase of kinetic energy closely depends on the growth rates of pressure and intrinsic properties of the systems, which causes the electron delocalization and metallization of the atoms. Different performances of metallization occur in high-pressure  $\text{CaH}_6$  and  $\text{NbH}_3$ , which is ascribed to their different metal atoms and other inherent properties. For the  $\text{CaH}_6$  system, under 200 GPa, the electronic delocalization of Ca and H atoms causes the formation of the equivalent covalent bonding between the H atoms. These pressure-induced delocalized covalent H–H bonds are weaker than the typical  $\sigma$ -bond in the  $\text{H}_2$  molecule, which aids in forming the metastable covalent H network. This extended H sublattice in  $\text{CaH}_6$  is a metallic-hydrogen-like structure featuring high energy density. In the  $\text{NbH}_3$  system, electron delocalization causes a certain degree of covalent character in Nb–H bonds and strong bonding between Nb atoms.

### 3.2. Energetic performance

The above discussion suggests that the MSHCs possess high energy. In the following section, the energetic performance of  $\text{CaH}_6$  and  $\text{NbH}_3$  has been well studied. Also, the relationship between their structural characteristics and energetic performance was explored theoretically by using thermodynamic and molecular dynamics methods.

#### 3.2.1. Basic properties

The energetic performance of energetic materials is closely related to their density, formation enthalpy and energy density. Higher density, higher positive formation enthalpy and higher energy density generally contribute to better energetic performance of explosives.<sup>[45]</sup> The densities ( $\rho$ ), formation enthalpies ( $\Delta H_f$ ) and energy density ( $E_d$ , numerically equal to detonation heat,  $Q$ ) of  $\text{CaH}_6$  and  $\text{NbH}_3$  under 200 GPa were calculated and listed in Table 1.

The  $\rho$  of  $\text{CaH}_6$  and  $\text{NbH}_3$  under 200 GPa are  $4.01$  g/cm<sup>3</sup> and  $10.08$  g/cm<sup>3</sup>, respectively. The high  $\rho$  of MSHCs is attributed to the high compact crystal structure compressed by high pressure and the inherent high mass of metal atoms. Their  $\Delta H_f$  values are respectively  $1020.98$  kJ/mol and  $468.92$  kJ/mol, both higher than that of CL-20, whose  $\Delta H_f$  is

a high positive value of  $377$  kJ/mol.  $\text{CaH}_6$  possesses a higher  $E_d$  of  $22.13$  kJ/g, which is 3.6 times that of CL-20 (a traditional energetic material, whose  $E_d$  is  $6.56$  kJ/g) and 2.3 times that of cubic gauche polymeric nitrogen (cg-N, a novel high-pressure energetic material, whose  $E_d$  is  $9.7$  kJ/g).<sup>[50]</sup> While, the  $E_d$  of  $\text{NbH}_3$  is comparable to that of TNT ( $4.184$  kJ/g<sup>[46]</sup>) but below CL-20. The outstanding  $E_d$  value of  $\text{CaH}_6$  is closely related to its structure and chemical bonding.  $\text{CaH}_6$  has a metallic-hydrogen-like structure with high H coordination and extended covalent H–H bonding induced by high pressure. This unique structure makes  $\text{CaH}_6$  in the metastable state and tends to store more energy introduced by high pressure within the H networks in the form of chemical energy. In contrast,  $\text{NbH}_3$  lacks the metallic-hydrogen-like structure and bonding features resembling  $\text{CaH}_6$ . Most of the energy introduced by high pressure is stored in the form of Coulomb energy. As a result,  $\text{NbH}_3$  has a relatively low  $E_d$  compared to  $\text{CaH}_6$ .

**Table 1.** Properties of high-pressure MSHCs.

Compound	Basic properties		Detonation performance			
	$\rho$ (g/cm <sup>3</sup> )	$\Delta H_f$ (kJ/mol)	$N$ (mol/g)	$Q$ ( $E_d$ ) (kJ/g)	$D$ (km/s)	$P$ (GPa)
$\text{CaH}_6^{\text{ideal (a)}}$	4.01	1020.98	0.0650	22.13	16.25	168.95
$\text{CaH}_6^{\text{MD (b)}}$	4.01	1020.98	0.0474	9.51	11.23	80.25
$\text{NbH}_3^{\text{ideal (a)}}$	10.18	468.92	0.0156	4.89	12.52	122.54
CL-20 <sup>pre. (c)</sup>	2.04	377	0.0308	6.56	9.62	44.1
CL-20 <sup>exp. (c)</sup>	2.04	$377.4 \pm 13$	–	6.1	9.6	43

(a) Parameters calculated based on the ideal case, (b) parameters calculated based on the MD simulation results, (c) predicted (via K–J equations) and experimental parameters for CL-20, Refs. [46–49]. Densities ( $\rho$ ), formation enthalpies ( $\Delta H_f$ ), energy density ( $E_d$ , numerically equal to detonation heat,  $Q$ ), gas production ( $N$ ), theoretical detonation heat ( $Q$ ), detonation velocity ( $D$ ), and detonation pressure ( $P$ ) are all included.

#### 3.2.2. Detonation performance

The K–J equations are a common method for predicting the detonation parameters of traditional CHON-based energetic materials, which have also been employed for metal-containing systems.<sup>[51]</sup> Here, we also borrowed the K–J equations to describe the detonation performance of MSHCs to a certain extent. The detonation parameters are closely related to the detonation reaction process and the corresponding final products. In an ideal case, the final products consist of metal crystal and  $\text{H}_2$  gas, in which the energy release reaches its optimal level. The corresponding detonation parameters were calculated and listed in Table 1, including the gas production ( $N$ ), theoretical detonation heat ( $Q$ ), detonation velocity ( $D$ ), and detonation pressure ( $P$ ).

The  $N$  of  $\text{CaH}_6$  and  $\text{NbH}_3$  are respectively  $0.0650$  mol/g and  $0.0145$  mol/g, due to the difference in their hydrogen content. The  $Q$  (numerically equal to  $E_d$ ) of  $\text{CaH}_6$  and  $\text{NbH}_3$  are respectively 5.3 times and 1.2 times TNT equivalent, and all

values for their  $D$  and  $P$  are higher than those of CL-20. Particularly, both the  $D$  and  $P$  of  $\text{CaH}_6$  are higher than those of  $\text{NbH}_3$  by over 30%, which is primarily attributed to its larger H content and the extra energy stored in its metallic-hydrogen-like structure, as discussed above. Thus, substantial amounts of high-temperature gases are released during its detonation, which provides the necessary force for working.

### 3.3. Decomposition behavior of $\text{CaH}_6$

As discussed above,  $\text{CaH}_6$  possesses metallic-hydrogen-like H–H covalent bonds and superior detonation performance. In this section, we further explored its energetic performance and potential applications by employing the *ab initio* molecular dynamics (AIMD) method and CP2K software. The decomposition process was theoretically simulated with a  $\text{CaH}_6$  model containing 112 atoms. The system was first optimized under 200 GPa and then was simulated for 3 ps within the NVT ensemble. To provide sufficient energy to initiate the decomposition, the thermostat temperature was set to 3000 K. The evolution of the potential energy and the structure throughout the decomposition simulation are shown in Fig. 2.

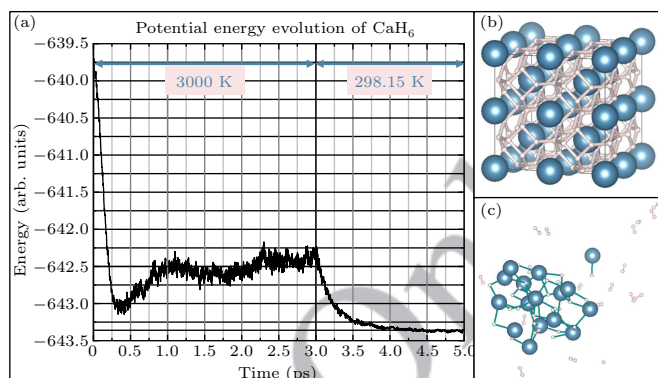


**Fig. 2.** Decomposition behavior of high-pressure  $\text{CaH}_6$ . (a) The potential energy evolution of the decomposition of  $\text{CaH}_6$ . (b) The structure of  $\text{CaH}_6$  before decomposition. (c) The products of the decomposition of  $\text{CaH}_6$ . The blue and white balls represent the Ca and H atoms, respectively. The pink and green bonds represent the H–H and Ca–H bonds, respectively.

After short time heating, the  $\text{CaH}_6$  system undergoes a rapid decomposition stage within 0.4 ps. During this stage, extensive bond dissociation occurs, accompanied by the release of hydrogen atoms and a sharp decline in potential energy. The freed H atoms further bond with neighboring H or Ca atoms to form  $\text{H}_2$  and  $\text{Ca}_n\text{H}_m$  clusters. At the end of this stage, 73% of H atoms form  $\text{H}_2$  molecules and the remaining 27% participate in the formation of  $\text{Ca}_n\text{H}_m$  clusters, as shown in Fig. 2(c). According to this simulated decomposition process, there is a decrease in both energy release and detonation parameters of  $\text{CaH}_6$  compared to the ideal case. Based on the potential energy decline throughout the simulations, the detonation parameters (denoted as  $\text{CaH}_6^{\text{MD}}$ ) were calculated and listed in Table 1. The results show that  $\text{CaH}_6$  exhibits large gas production ( $N^{\text{MD}} = 0.0474$  mol/g, or 1062.26 mL/g), also

far exceeding that of CL-20 (628.5 mL/g.<sup>[52]</sup>). The  $Q^{\text{MD}}$  is 9.51 kJ/g, which is 2.3 times that of TNT. The  $D^{\text{MD}}$  and  $P^{\text{MD}}$  are 11.23 km/s and 80.25 GPa, respectively. Consequently, Table 1 shows the detonation performance of  $\text{CaH}_6$  in different decomposition processes, the  $N$ ,  $Q$ ,  $D$  and  $P$  respectively lie in (0.65–0.474 mol/g), (22.13–9.51 kJ/g), (16.25–11.23 km/s) and (168.95–80.25 GPa), which are all higher than those of CL-20. Our simulation validates the excellent detonation performance of  $\text{CaH}_6$  and its tremendous potential as high explosives.

The above discussion about the hydrogen release suggests the potential of  $\text{CaH}_6$  for high-performance propellant component. Further, its combustion performance was predicted by using the Explo 5 software. The theoretical vacuum specific impulse ( $I_{\text{sp}}$ ) of  $\text{CaH}_6$  is 490.66 s, which is 1.9 times that of hexogen (RDX, whose  $I_{\text{sp}}$  is 258 s)<sup>[53]</sup> and 3.2 times that of ammonium perchlorate (AP, whose  $I_{\text{sp}}$  is 155 s).<sup>[54]</sup> The characteristic velocity ( $c^*$ ) and the combustion temperature of  $\text{CaH}_6$  are 2672.4 m/s and 2620.7 K, respectively. The main combustion products consist of 24.54% Ca and 71.76%  $\text{H}_2$ , corresponding to a hydrogen release ratio of 97.48%. All these results highlight that high-pressure  $\text{CaH}_6$  exhibits combustion performance far exceeding that of common high-energy propellant components such as RDX and AP, suggesting its potential for propellants.

## 4. Conclusion

For the first time,  $\text{CaH}_6$  and  $\text{NbH}_3$  were chosen as examples of MSHCs to systematically investigate their energetic performance. Since the two MSHCs were obtained under high pressure, both the potential and kinetic energy of the systems increase, while the increase in kinetic energy is more rapid than the Coulomb energy as the pressure rises. Consequently, both MSHCs exhibit high energy densities, with the values of 5.3 times and 1.2 times that of TNT, respectively. Notably, the outstanding energy density of  $\text{CaH}_6$  is relatively higher than that of  $\text{NbH}_3$ , which is closely related to the structure and characteristic H–H covalent bonds in  $\text{CaH}_6$ .  $\text{CaH}_6$  possesses highly ordered extended H sublattice and metastable covalent H network with strong pressure-induced covalent H–H bond, which are similar to those in metallic hydrogen and offer  $\text{CaH}_6$  higher energy density.

Given this, we conducted an in-depth study of its detonation process and energy release performance. First of all, instead of the complete decomposition into pure Ca metal and  $\text{H}_2$ ,  $\text{CaH}_6$  might undergo complex reactions and produce various  $\text{Ca}_n\text{H}_m$  clusters. Furthermore, the corresponding energy density of  $\text{CaH}_6$  was predicted as 2.3 times TNT equivalent. Consequently, the theoretical energy density of  $\text{CaH}_6$  ranges from 2.3 to 5.3 times TNT equivalent. Moreover, at least 72.9% of H atoms in  $\text{CaH}_6$  are finally released to form 35

H<sub>2</sub> molecules in the rapid energy-release stage, suggesting its potential for high-performance propellant component. Therefore, we further predicted its combustion performance. The theoretical specific impulse, characteristic velocity and hydrogen release ratio of CaH<sub>6</sub> are respectively 490.66 s, 2672.4 m/s and 97.48%, indicating its superior combustion performance far exceeding that of common high-energy propellant components such as RDX and AP.

Our results demonstrate that the energy density and energy release of high-pressure MSHCs are significantly higher than traditional CHON-based explosives, which makes them a promising candidate for next-generation energetic materials. Certain high-pressure MSHCs, such as CaH<sub>6</sub>, possess metallic-hydrogen-like structures and characteristic covalent bonds and can release substantial amounts of high-temperature gases during their detonation, demonstrating tremendous potential for explosives and high-energy propellant components. To date, stabilizing MSHCs, which are synthesized at high pressure, under ambient pressure conditions is very challenging. Using the pressure-quench protocol (PQP) or achieving solid solutions is promising to recover the pressure-induced phases to ambient pressure, which may extend the research on MSHCs from basic studies to applied research. This study enhanced the chemical understanding of MSHCs and provided a new route to design novel high-energy-density materials, promoting the exploration of MSHCs in defense, aerospace, and energy sectors.

## References

- [1] Wigner E and Huntington H 1935 *The Journal of Chemical Physics* **3** 764
- [2] Ashcroft N W 1968 *Phys. Rev. Lett.* **21** 1748
- [3] Nellis W 1999 *Philosophical Magazine B* **79** 655
- [4] Isaac F S and John W C 2010 *J. Phys.: Conf. Ser.* **215** 012194
- [5] McMahon J M and Ceperley D M 2011 *Phys. Rev. B* **84** 144515
- [6] Dias R P and Silvera I F 2017 *Science* **355** 715
- [7] Ashcroft N 2004 *Phys. Rev. Lett.* **92** 187002
- [8] Duan D, Liu Y, Tian F, Li D, Huang X, Zhao Z, Yu H, Liu B, Tian W and Cui T 2014 *Scientific Reports* **4** 6968
- [9] Drozdov A, Eremets M, Troyan I, Ksenofontov V and Shylin S I 2015 *Nature* **525** 73
- [10] Abe K 2017 *Phys. Rev. B* **96** 144108
- [11] Somayazulu M, Ahart M, Mishra A K, Geballe Z M, Baldini M, Meng Y, Struzhkin V V and Hemley R J 2019 *Phys. Rev. Lett.* **122** 027001
- [12] Ma L, Wang K, Xie Y, Yang X, Wang Y, Zhou M, Liu H, Yu X, Zhao Y and Wang H 2022 *Phys. Rev. Lett.* **128** 167001
- [13] Luo Y X, Gao J, Liu Q J, Fan D H and Liu Z T 2024 *Journal of Molecular Modeling* **30** 229
- [14] Miao M, Sun Y, Zurek E and Lin H 2020 *Nature Reviews Chemistry* **4** 508
- [15] Sun Y and Miao M 2023 *Chem* **9** 443
- [16] Tarasov B P, Bocharnikov M S, Yanenko Y B, Fursikov P V, Minko K B and Lototsky M V 2020 *J. Phys.: Energy* **2** 024005
- [17] Wu X L, Xu S, Pang A M, Cao W G, Liu D B, Zhu X Y, Xu F Y and Wang X 2021 *Defence Technology* **17** 1262
- [18] Bezudnyy A, Blinov D and Dunikov D 2023 *Journal of Energy Storage* **68** 107590
- [19] Makhov M 2024 *Russian Journal of Physical Chemistry B* **18** 185
- [20] Li Z, He X, Zhang C, Wang X, Zhang S, Jia Y, Feng S, Lu K, Zhao J and Zhang J 2022 *Nat. Commun.* **13** 2863
- [21] He X, Zhang C, Li Z, Zhang S, Min B, Zhang J, Lu K, Zhao J, Shi L and Peng Y 2023 *Chin. Phys. Lett.* **40** 057404
- [22] He X, Zhang C, Li Z, Lu K, Zhang S, Min B, Zhang J, Shi L, Feng S and Liu Q 2024 *Materials Today Physics* **40** 101298
- [23] Banacký P and Noga J 2021 *J. Appl. Phys.* **130** 183902
- [24] Hou P, Huo Z and Duan D 2023 *The Journal of Physical Chemistry C* **127** 23980
- [25] Denchfield A, Park H and Hemley R J 2024 *Proc. Natl. Acad. Sci. USA* **121** e2413096121
- [26] Sun Y, Zhong X, Liu H and Ma Y 2024 *National Science Review* **11** nwad270
- [27] Kresse G and Furthmüller J 1996 *Computational Materials Science* **6** 15
- [28] Kresse G and Furthmüller J 1996 *Phys. Rev. B* **54** 11169
- [29] Blochl P E 1994 *Phys. Rev. B* **50** 17953
- [30] Perdew J P, Burke K and Ernzerhof M 1996 *Phys. Rev. Lett.* **77** 3865
- [31] Dudarev S L, Botton G A, Savrasov S Y, Humphreys C and Sutton A P 1998 *Phys. Rev. B* **57** 1505
- [32] Solovyev I V, Dederichs P H and Anisimov V I 1994 *Phys. Rev. B* **50** 16861
- [33] Grimme S, Antony J, Ehrlich S and Krieg H 2010 *The Journal of Chemical Physics* **132** 154104
- [34] Momma K and Izumi F 2011 *Journal of Applied Crystallography* **44** 1272
- [35] Maintz S, Deringer V L, Tchougreeff A L and Dronskowski R 2016 *Journal of Computational Chemistry* **37** 1030
- [36] Kamlet M J and Jacobs S 1968 *The Journal of Chemical Physics* **48** 23
- [37] Hutter J, Iannuzzi M, Schiffmann F and VandeVondele J 2014 *Wiley Interdisciplinary Reviews: Computational Molecular Science* **4** 15
- [38] VandeVondele J and Hutter J 2003 *The Journal of Chemical Physics* **118** 4365
- [39] Zhao D, Liu S, Rong C, Zhong A and Liu S 2018 *ACS Omega* **3** 17986
- [40] VandeVondele J and Hutter J 2007 *The Journal of Chemical Physics* **127** 114105
- [41] Chesnut D B 2000 *The Journal of Physical Chemistry A* **104** 11644
- [42] Dronskowski R and Blochl P E 1993 *The Journal of Physical Chemistry* **97** 8617
- [43] Deringer V L, Tchougreeff A L and Dronskowski R 2011 *The Journal of Physical Chemistry A* **115** 5461
- [44] Ashcroft N W, Mermin N D and Rodriguez S 1978 *American Journal of Physics* **46** 116
- [45] Robertson R 1921 *Journal of the Chemical Society, Transactions* **119** 1
- [46] Meyer R, Kohler J and Homburg A 2016 *Explosives* 7th Ed. (Weinheim: Wiley-VCH)
- [47] Politzer P and Murray J S 2011 *Central European Journal of Energetic Materials* **8** 209
- [48] Simpson R, Urtiew P, Ornellas D, Moody G, Scribner K and Hoffman D 1997 *Propellants, Explosives, Pyrotechnics* **22** 249
- [49] Muravyev N V, Monogarov K A, Melnikov I N, Pivkina A N and Kiselev V G 2021 *Physical Chemistry Chemical Physics* **23** 15522
- [50] Yin K, Wang Y, Liu H, Peng F and Zhang L 2015 *Journal of Materials Chemistry A* **3** 4188
- [51] Huang B, Wang B, Wu S, Guogan F, Hu W and Frapper G 2021 *Chemistry of Materials* **33** 5298
- [52] He S, Zhang L, Heng S, Liu Z and Shi Z 2007 *Energetic Materials* **15** 515
- [53] Liu D, Chen J, Yang R, Xiao L, Zhang G, Feng X, Zhang K, Jiang W and Hao G 2024 *Chemistry of Materials* **36** 3496
- [54] Klapotke T M 2018 *Energetic Materials Encyclopedia* (Berlin: De Gruyter)